Composite scaffold provides a cell delivery platform for cardiovascular repair

Amandine F. G. Godier-Furnémont[a], Timothy P. Martens[a,b], Michael S. Koeckert[a], Leo Wan[a], Jonathan Parks[a], Kotaro Arai[c], Geping Zhang[b], Barry Hudson[b], Shunichi Homma[c], and Gordana Vunjak-Novakovic[a,1]

[a]Department of Biomedical Engineering, Columbia University, New York, NY 10032; and Departments of [b]Surgery and [c]Medicine, Columbia University Medical Center, New York, NY 10032

Edited by Robert Langer, Massachusetts Institute of Technology, Cambridge, MA, and approved March 31, 2011 (received for review March 22, 2011)

Control over cell engraftment, survival, and function remains critical for heart repair. We have established a tissue engineering platform for the delivery of human mesenchymal progenitor cells (MPCs) by a fully biological composite scaffold. Specifically, we developed a method for complete decellularization of human myocardium that leaves intact most elements of the extracellular matrix, as well as the underlying mechanical properties. A cell–matrix composite was constructed by applying fibrin hydrogel with suspended cells onto decellularized sheets of human myocardium. We then implanted this composite onto the infarct bed in a nude rat model of cardiac infarction. We next characterized the myogenic and vasculogenic potential of immunoselected human MPCs and demonstrated that in vitro conditioning with a low concentration of TGF-β promoted an arteriogenic profile of gene expression. When implanted by composite scaffold, preconditioned MPCs greatly enhanced vascular network formation in the infarct bed by mechanisms involving the secretion of paracrine factors, such as SDF-1, and the migration of MPCs into ischemic myocardium, but not normal myocardium. Echocardiography demonstrated the recovery of baseline levels of left ventricular systolic dimensions and contractility when MPCs were delivered via composite scaffold. This adaptable platform could be readily extended to the delivery of other reparative cells of interest and used in quantitative studies of heart repair.

biomaterial | cardiac repair | human stem cell | cardiac patch

Given the adult heart's minimal capacity for endogenous regeneration (1), cell therapy has emerged as a viable option for revascularization (2) and regeneration (3) of the infarct bed. Cell delivery methods are progressing through clinical trials, particularly in the setting of end-stage heart failure, where the lack of effective therapies leads to more than 500,000 deaths per year in the United States alone (4). Human mesenchymal stem cells (MSCs) were used with variable functional improvement and neovascularization (5–10). This outcome is thought to be largely due to the use of cell suspensions that are limited by poor cell retention (11), survival (12), engraftment (13), and differentiation (14). The underlying mechanisms (i.e., secretion of paracrine factors vs. cell incorporation) are not well defined and can be interrogated only through control over cell retention (e.g., by the use of scaffolding materials) and insight into cell phenotype (e.g., expression of functional markers). We introduce a cell delivery platform that combines a fully biological gel–matrix composite scaffold with biochemical preconditioning of human MPCs. The resulting vasculogenic and myogenic cell properties and functional benefits of the cell delivery platform were evaluated in an animal model of myocardial infarction (MI).

Results and Discussion

Cell Delivery Platform. Composite scaffolds for cell delivery were assembled from thin sheets of decellularized human myocardium and fibrin hydrogel. MPCs were immunoselected from bone marrow aspirates using STRO-1 and STRO-3 and culture-expanded to passage 5. The resulting cells were cultured in vitro with or without TGF-β conditioning, suspended in fibrin, and delivered into the decellularized matrix. Composite scaffolds containing STRO-3 MPCs and cell-free scaffolds were studied in nude rat models of acute and chronic cardiac infarction (Fig. 1*A*).

Our hypothesis was that the preserved architecture, biomechanics, and largely retained composition of the actual cardiac matrix will impose long-range order to seeded cells (15) and restore the physiological microenvironment with cell differentiation cues (16). Cells were delivered into the decellularized matrix using rapidly gelling fibrin, a widely used tunable biological material with vasculogenic properties (17). In the composite, decellularized myocardium provides a structural and biomechanical template with long-range signaling, whereas fibrin enables cell retention and local signaling. The composite scaffold can retain sutures when attached to the infarct bed and is sufficiently pliable to be molded over the surface of the heart.

Based on previous work (18–21), we developed a method for complete decellularization of human myocardium. Human myocardium was obtained from surgical explants, and decellularization was achieved using heart sections from patients with both ischemic and nonischemic cardiomyopathies. Notably, decellularization of slices from infarcted regions of ischemic hearts, which were not used in experiments, was markedly more difficult to achieve. For all implantation studies, slices obtained from nonischemic myocardium were chosen, to retain as much of the normal tissue structure as possible (Fig. S1 *A* and *B*), and were used to make 300 ± 50-μm-thick scaffolds for cell delivery. The decellularization protocol that we developed (lysis for 2 h, detergent for 6 h, DNase/RNase for 3 h) consistently removed 99.5% ± 0.3% of the nuclear material (Fig. S1*D*). The application of 0.5% SDS was followed by extensive rinsing of decellularized tissue to remove any residual SDS, which could damage the extracellular matrix and seeded cells. The use of thin tissue sections enabled thorough removal of SDS, such that no adverse effects on the seeded cells were observed.

Cardiomyocyte orientation within the ventricular wall is highly anisotropic (22), and the architecture of decellularized matrix depends in large part on the direction of sectioning (Fig. 1 *B–F*). SEM revealed low porosity and closed pores in apex-to-base (Fig. 1*C*) and radial sections (Fig. 1*D*). In contrast, circumferential sections (Fig. 1 *E* and *F*) contained large interconnected pores and smooth channels (Fig. S1*C*) corresponding to intramyocardial arterioles that could facilitate oxygen transport and serve as precursors for new blood vessels. Because circumferential sections enabled rapid infiltration of cells and fluid, via pores oriented perpendicular to the infarct surface, only these sections were used to create scaffolds.

In the decellularized matrix, type I collagen backbone, collagen IV, laminin, and vitronectin (Fig. 1 *G–I*) maintained their original presence, whereas fibronectin was lost from the whole

Author contributions: A.F.G.G.-F., T.P.M., and G.V.-N. designed research; A.F.G.G.-F, T.P.M., M.S.K., J.P., K.A., G.Z., and B.H. performed research; A.F.G.G.-F., T.P.M., L.W., K.A., S.H., and G.V.-N. analyzed data; and A.F.G.G.-F., T.P.M., and G.V.-N. wrote the paper.

The authors declare no conflict of interest.

This article is a PNAS Direct Submission.

[1]To whom correspondence should be addressed. E-mail: gv2131@columbia.edu.

This article contains supporting information online at www.pnas.org/lookup/suppl/doi:10.1073/pnas.1104619108/-/DCSupplemental.

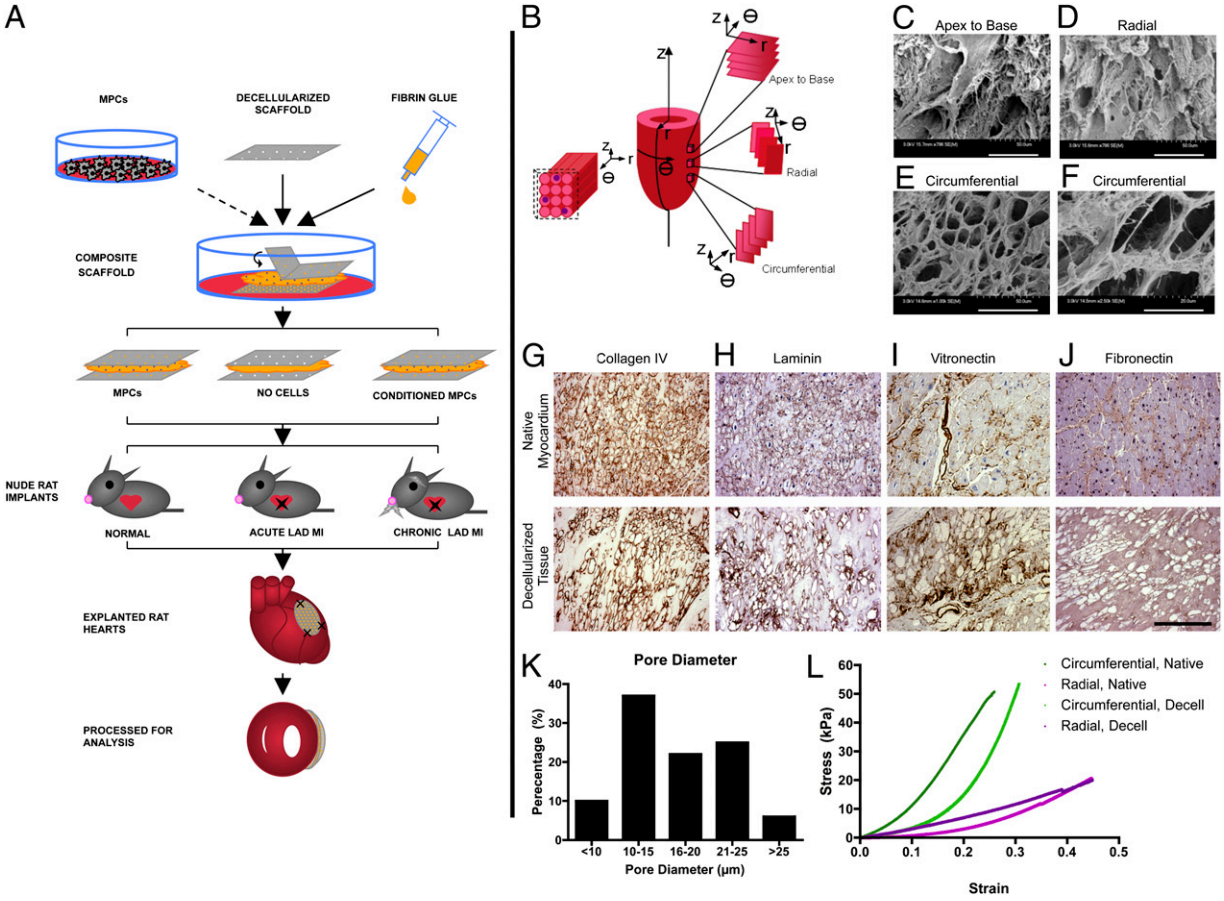

Fig. 1. Cell delivery platform. (*A*) Composite scaffolds assembled from thin sheets of decellularized human myocardium and fibrin hydrogel were seeded with MPCs, cultured in vitro with or without TGF-β conditioning, and implanted into nude rat models of acute and chronic ischemia. After 4 wk, heart function was evaluated by echocardiography ex vivo analyses. (*B*) The three axes of the heart (*r*, *q*, and *z*), the directions for sectioning (apex to base, circumferential, and radial), and the short axis of myocytes seen in circumferential sections. (*C–F*) Scanning electron micrographs of decellularized scaffolds: apex to base sections (*C*; 796×), radial sections (*D*; 986×), and circumferential sections (*E*; 1,000×; *F*, 2,500×). (*G–J*) Staining of extracellular matrix components circumferential sections of native and decellularized tissue: collagen IV (*G*), laminin (*H*), vitronectin (*I*), and fibronectin (*J*). (Scale bar: 250 μm.) (*K*) Average pore diameters in decellularized scaffolds. (*L*) Similar properties of native (circumferential, blue; radial, pink) and decellularized (circumferential, green; radial, purple) tissue measured in uniaxial tensile tests (tensile moduli calculated at 20% strain).

regions of the extracellular matrix, resulting in patchy immunostaining of the decellularized matrix (Fig. 1*J*). Laminin and collagen IV remained localized to the myocyte pores and coronary vessel basement membranes, and vitronectin remained localized to blood vessels. Decellularized myocardial sheets maintained the properties of a relaxed native tissue. The majority of pores were in the 10- to 25-μm diameter range (average diameter, 16.7 ± 3.5 μm; Fig. 1*K*). For circumferential sections tested in cardioplegic solution at 20% strain, the tangential modulus of native matrix was 272.9 ± 15 kPa and that of decellularized matrix was 224.0 ± 37 kPa (Fig. 1*L*).

Phenotype Characterization of Human MPCs. Populations of MPCs were derived from bone marrow by immunoselection for STRO-3 (23), expanded up to passage 5, and evaluated for expression of developmental, myogenic, and vascular markers (Fig. 2 *A–C*). At all passages, these cells demonstrated high levels of mRNA for several developmentally relevant receptors, including BMPR1, BMPR2, FGFR1, Fzd1, and Fzd2 (Fig. 2*A*). Expression was stable for all myogenic markers except Islet1, which showed expression at passage 2 but not at passage 5. Of note, the cardiac-specific markers Nkx2.5 and GATA4 were not expressed at passage 2 or 5, whereas Mef2C, GATA6, and Tbx5 were expressed slightly less at passage 5 than at passage 2 (Fig. 2*B*). In contrast to the low expression levels of myogenic markers, significant up-regulation of vascular cytokines, receptors, and structural proteins was observed between the passage 2 and passage 5 (Fig. 2*C*). Specifically, mRNA for angiogenic factors SDF-1, angiopoietin, and endothelin was up-regulated by 2.1-, 2.6-, and 11.3-fold, respectively. The expression of endothelin receptors A and Flt1 increased by 5.7- and 2.0-fold, respectively. Vascular smooth muscle markers also were up-regulated between passage 2 and passage 5, including α-smooth muscle actin (SMA) by 3.7-fold, myocardin by 7.5-fold, and connexin 43 by 2.5-fold. We used these data to select passage 5 MPCs for all experiments, based on their enhanced vascular profile and the maintenance of most developmental and myogenic markers.

Effects of TGF-β Conditioning in Vitro on MPC Phenotype. TGF-β has been implicated in vascular homeostasis, angiogenesis, and vascular morphogenesis (24), with affinity for multiple receptors of the TGF-β superfamily (25). We sought to determine the biological consequences of TGF-β conditioning on the vasculogenic and myogenic profiles of MPCs. Consistent with a previous report (26), intermediate (1 ng/mL) and high (10 ng/mL) concentrations of TGF-β resulted in significant up-regulation of osteochondral genes, including osteopontin, osterix, type X collagen, and aggrecan (Fig. 2 *D–G*). In contrast, low concentrations (0.1 ng/mL) of TGF-β was associated with decreased osteopontin and aggrecan mRNA, no change in osterix or type X collagen message, and increased Flt-1 and VCAM expression (Fig. 2 *H* and *I*). Although MPCs expressed myogenic genes early

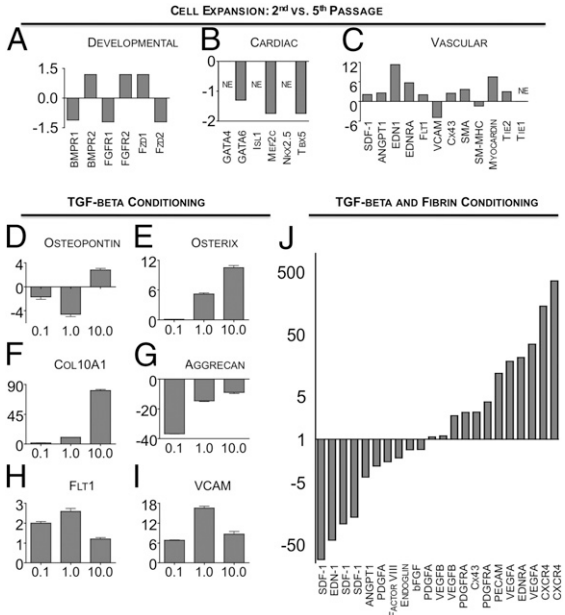

Fig. 2. Genotypic and phenotypic profiles of immunoselected human MPCs. (*A–C*) STRO-3–immunoselected MPCs (obtained from Angioblast Systems) were expanded up to passage 5. RT-PCR of MPCs to analyze genotypic profiles for (*A*) developmental markers (FC; passages 2–5), (*B*) cardiac markers (FC; passages 2–5), and (*C*) vasculogenic markers (FC; passages 2–5). (*D–J*) Cells cultured with TGF-β supplementation at passage 5 were analyzed for changes in osteochondral markers (*D–G*) and vasculogenic markers (*H* and *I*). Gene expression of vascular markers (many with more than one gene probe per transcript or variant) in STRO-1–immunoselected MPCs conditioned in TGF-β and cultured in fibrin with TGF-β supplementation are shown on a log scale (*J*). All charts are plotted with the *y*-axis as FC. Markers with no expression are denoted by "NE."

in culture, their overall profile was vasculogenic. MPCs express smooth muscle markers (α-SMA, Cx-43, and endothelin receptor A) and endothelial-associated markers (VCAM and Flt1), yet lack smooth muscle myosin heavy chain and Tie1. This vasculogenic profile was well maintained and further augmented by serial cell passage at low TGF-β concentrations.

Effects of Scaffold on MPC Phenotype. We independently confirmed the vascular profile of MPCs for bone marrow-derived cells immunoselected for STRO-1, an alternative to STRO-3 (27) that is not commercially available. STRO-1 selected MPCs also were expanded to passage 5, cultured with or without TGF-β for 7 d, and encapsulated in fibrin hydrogel (10^6 cells/300 μL), following the same protocol used in creating composite scaffolds for in vivo implantation. Gene array analysis of these cells that were conditioned or not conditioned with TGF-β and encapsulated or not encapsulated in fibrin showed a vasculogenic profile comparable to that seen for the STRO-3 population.

The TGF-β–conditioned cells in fibrin showed significant up-regulation of numerous markers (many of which were evaluated with more than one probe per gene transcript or variant), as evidenced by the fold change calculated against the MPCs not conditioned with TGF-β or fibrin (Fig. 2*J*). For these cells, we found significant up-regulation of VEGFA (34.7- and 18.3-fold), VEGFB (1.15- and 1.10-fold), and a panel of angiogenic markers including the endothelin receptor A (21.1-fold), PECAM (11.8-fold), PDGF receptor B (2.4-fold), PDGF receptor A (4.0- and 2.7-fold), and Connexin 43 (2.76-fold). We also measured significant down-regulation of other factors, including basic FGF (−1.5-fold), PDGFA (−1.5- and −2.7-fold), and the angiogenic markers endothelin 1 (−42.5- fold), angiopoeitin 1 (−4.1-fold), factor VIII (−2.3-fold), and endoglin (−2.0-fold). Importantly, the decreased expression of SDF-1 (−87-, −23-, and −18-fold) and increased expression of its cognate receptor CXCR4 (140- and 359-fold) were among the largest changes seen in the cells after TGF-β conditioning and fibrin encapsulation.

Effects of Cell Delivery Platform in Rodent Models of Acute and Chronic MI. We performed two independent in vivo studies. The first study was designed to evaluate the migratory and provascular effects of our delivery platform by investigating TGF-β–conditioned MPCs delivered in composite scaffold, nonconditioned MPCs delivered in composite scaffold (control for TGF-β), and composite scaffold only (control for MPCs and TGF-β). Each group was studied in two models of MI, acute (patch implanted at the time of MI) and chronic (patch implanted at 4 wk post-MI), as well as in normal myocardium (control for MI). The second study was designed to measure the functional benefits of the best composite scaffold group from the first study, the TGF-β–conditioned MPCs delivered in composite scaffold. The functional outcomes were determined for the TGF-β–conditioned MPCs delivered in composite scaffold and two controls, MPCs injected with saline solution (control for scaffold) and a no-treatment group. Rats were implanted with the TGF-β–conditioned MPC composite scaffold or injected with MPC at 7 d post-MI and evaluated at 28 d after treatment by echocardiography and endpoint histological and molecular assays.

Cell Delivery via Composite Scaffolds into Acute and Chronic MI Models. In our first in vivo study, the regenerative capacity of MPCs was evaluated at 4 wk after implantation in the acute (immediately after MI) and chronic (4 wk post-MI) nude rat MI models. Three groups were studied: (*i*) MPCs conditioned with TGF-β and seeded into scaffold ($n = 7$ acute, $n = 4$ chronic, $n = 4$ normal), (*ii*) MPCs seeded into scaffold (control for TGF-β; $n = 7$ acute, $n = 4$ chronic, $n = 4$ normal), and (*iii*) scaffold alone (control for MPCs; $n = 7$ acute). The open scaffold pores enabled infiltration of fluid and cells into the scaffold, as well as cell migration from the scaffold into the infarct bed. At 4 wk postimplantation, all experimental groups demonstrated physical integration into the underlying host myocardium.

In the acute MI model, TGF-β and MPCs markedly enhanced angiogenesis and arteriogenesis in the infarct bed, as evidenced by the increased size and frequency of blood vessels positive for factor VIII and SMA. The number of factor VIII-positive vessels per view field (an indicator of angiogenesis) was 21.3 ± 5.1 for the TGF-β/MPC/scaffold group, 14.7 ± 5.4 for the MPC/scaffold group, and 9.8 ± 4.4 for the scaffold-only group ($P < 0.05$; Fig. 3 *A–D*). The number of SMA-positive vessels per view field (an indicator of arteriogenesis) was 10.5 ± 2.4 for the TGF-β/MPC/scaffold group, 7.2 ± 3.4 for the MPC/scaffold group, and 3.5 ± 2.0 for the scaffold-only group ($P < 0.05$; Fig. 3 *E–H*). TGF-β conditioning significantly increased the number of human MPCs within the infarct bed (6.5 ± 5.2 vs. 0.6 ± 0.7 MPCs per view field; $P < 0.05$), with a trend toward fewer MPCs remaining within the patch (1.2 ± 1.9 vs. 2.2 ± 2.7 MPCs per view field) (Fig. 3*I*). Human MPCs were often found in close proximity to endogenous vessels (Fig. 3 *J* and *K*), but did not appear to contribute to either endothelial or intramural components, instead occupying a perivascular position.

We further evaluated the TGF-β/MPC/scaffold group and the MPC/scaffold group in models of acute MI (Fig. 3*L*) and chronic MI (Fig. 3*M*), as well as in normal myocardium (Fig. 3 *N* and *O*). Greater cell migration into the infarct bed was observed for TGF-β–conditioned MPCs than for nonconditioned MPCs, as evidenced by the higher numbers of cells per view field. (Yellow arrows indicate cell clusters; high-magnification views of the individual cell clusters are shown in the insets.) TGF-β/MPC density in the infarct bed (Fig. 3*M*) was markedly lower in the chronic MI model than in the acute MI model (3.6 ± 2.5 vs. 6.5 ± 5.2 MPCs per view field; $P < 0.05$; Fig. 3*P*). Virtually no migration of MPCs into healthy myocardium was observed (Fig. 3*O*). Consistent with the observed differences between the acute MI and chronic MI models, regions of inflammation, such as chest wall adhesions (Fig. 3*N*) and microinfarctions caused by

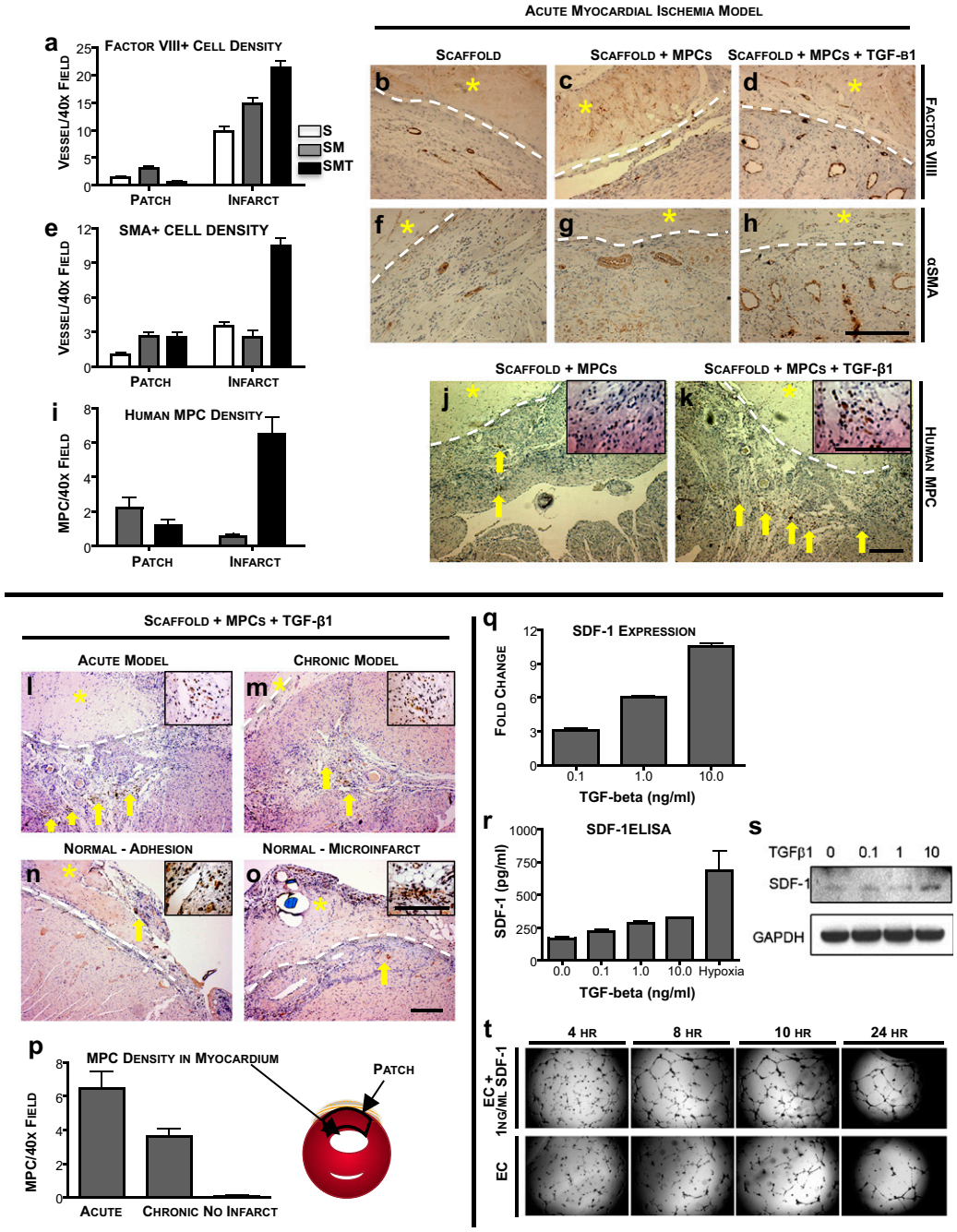

Fig. 3. Implantation of the composite constructs in nude rat models of acute and chronic cardiac infarction. The in vivo groups were designated the TGF-β/MPC/scaffold group (SMT), MPC/scaffold group (SM), and scaffold only group (S). (*A–K*) Acute infarction model. Representative data at 4 wk post-implantation, for factor VIII–positive vessels (*A–D*), SMA-positive vessels (*E–H*), and the presence of MPCs (*I–K*) for each group. (*L–P*) Presence of TGF-β–conditioned MPCs on scaffolds in acute infarction, chronic infarction, and noninfarction models at 4 wk after implantation. (*Q*) RT-PCR of TGF-β–conditioned MPCs (passage 5), shown as FC in SDF-1 expression relative to baseline (cells not conditioned with TGF-β). (*R*) ELISA of supernatants from MPCs after culture with or without TGF-β and with or without hypoxia. (*S*) Western blot analysis demonstrating SDF-1 protein expression. (*T*) Matrigel assay of coronary endothelium with (*Upper*) and without (*Lower*) SDF-1 supplementation. Patches over the rat hearts are denoted by a yellow asterisk, and the interface is indicated by a dotted white line. Data are shown as average ± SEM. (Scale bars: 250 μm.)

sutures (Fig. 3*O*), served as powerful stimuli for MPC migration. (Fig. S3 provides high-magnification images of these views.)

Consistent with previous reports that MPCs expressing STRO-1 and STRO-3 show greater SDF-1 gene and protein expression (27–29), RT-PCR analysis of passage 5 MPCs demonstrated strong expression and concentration-dependent increase of SDF-1 message with TGF-β supplementation (Fig. 3*Q*), along with increased SDF-1 protein expression (Fig. 3*S*). ELISA of supernatants (Fig. 3*R*) revealed constitutive SDF-1 release by MPCs, which was further enhanced by TGF-β conditioning. MPC culture under hypoxic conditions demonstrated the greatest release of SDF-1, suggesting that the capacity for SDF-1 release could be recovered upon cell migration into the ischemic infarct bed. In addition, the supplementation of exogenous SDF-1 to coronary endothelium enhanced and stabilized endothelial network formation (Fig. 3*T*).

Notably, despite the cardiac nature of the MPC environment after implantation, there was no evidence of MPC differentiation into cardiomyocytes in either the patch or the native myocar-

dium. In fact, we found no evidence of differentiation into either vascular structures or myocytes, consistent with the lack of incorporation of MSCs into engineered blood vessels (30). Rather, MPCs were found clustered in a perivascular location similar to the "niche" that they occupy in bone marrow (31). These observations support the notion that paracrine factors and up-regulation of endogenous neovascularization are the primary mechanisms of repair seen with MSCs (32), and that the differentiation of these cells into cardiomyocytes in vivo is unlikely (33). These data also support the notion that an acute infarct, which is still in the healing phase, represents a more favorable substrate for cell-based repair than a chronic infarct that has progressed to a fibrous scar (34).

Evaluation of Left Ventricular Function. In the second in vivo study, we evaluated the functional consequences of MPC implantation by echocardiography. Baseline analysis at 3 d after left anterior descending artery (LAD) ligation (n = 45) demonstrated increased left ventricular diastolic and systolic diameters (LVDd and LVDs) and area (LVDA and LVSA), and decreased fractional shortening (FS) and fractional area change (FAC) (Fig. 4 *A*–*F* and Fig. S2 *A*–*F*) that normally occur after infarction. Animals with FS ≤45% (n = 35) were randomized to receive treatment at 7 d after LAD ligation, and the effects were evaluated after a period of 4 wk. At the endpoint, the groups were no treatment (n = 10), TGF-β–conditioned MPCs (n = 9), and TGF-β–conditioned MPCs in a composite scaffold (n = 8).

In untreated animals, LVDd (Fig. 4*A*), LVDA (Fig. 4*B*), LVDs (Fig. 4*C*), and LVSA (Fig. 4*D*) continued to increase, whereas FS (Fig. 4*E*) and FAC (Fig. 4*F*) decreased, indicating left ventricular dilatation and loss of contractility. Delivery of TGF-β–conditioned MPCs, either by intramyocardial injection or in a composite scaffold, had no significant effect on diastolic dimensions (Fig. 4 *A* and *B*). Whereas intramyocardial injection of MPCs attenuated the increase in systolic dimensions (Fig. 4 *C* and *D*) and preserved post-MI FS and FAC (Fig. 4 *E* and *F*), only the MPC delivery via composite scaffold resulted in significant preservation of LVDA (Fig. 4*D*) and FAC (Fig. 4*F*).

Interestingly, our echocardiography results mirror those reported by Eschenhagen's group (35) despite the use of different conditioning regimens (biological vs. mechanical) and cell sources (human MPCs vs. neonatal rat myocytes). Both therapies preserved the functional state of the myocardium at the time of intervention and attenuated remodeling rather than return of the ventricle to its normal baseline. Thus, in cell therapy, preservation of chamber geometry and inhibition of deterioration may be a more realistic endpoint than functional improvement. These findings also support cell therapy as a preventive measure in early heart failure rather than a "last resort" treatment for end-stage ventricles where there is little left to salvage.

Effects of Delivery Platform on MPC Function. We hypothesized that the observed selective migration of MPCs into the infarct bed—but not into the healthy myocardium—can be attributed, at least in part, to the SDF-1/CXCR4 axis. By binding to its cognate receptor CXCR4, SDF-1 stimulates cell growth, proliferation, antiapoptosis, migrational and transcriptional activation, and cell recruitment and retention in the repair zone (36–38). In an infarcted heart, the up-regulation of VEGF by hypoxia and inflammation induces downstream expression of SDF-1 that captures the recruited cells presenting CXCR4, providing a central mechanism for regulation of adult angiogenesis (39). In this way, the SDF-1/CXCR4 axis plays a key role in directing the migration of the CXCR4-expressing cells from bone marrow to blood and injured myocardium (40–43).

In a tissue engineering application using a prevascularized patch, the inclusion of prosurvival and angiogenic factors, including SDF-1 to mobilize bone marrow stem cells, preserved chamber geometry and function (44). Beyond the first few days after MI, the SDF-1 gradients for stem cell mobilization into the infarct bed are unfavorable, due to the decreased SDF-1 levels in myocardium (45). However, this decrease can be reversed by injection of MSCs, which then recruit the additional bone marrow cells into the infarct zone (45) and enhance the survival and function of border zone cardiomyocytes (46).

In previous studies, bone marrow cells delivered to human patients were more responsive to SDF-1 during acute MI than at a normal baseline (10). Normal myocardium is not expected to produce a gradient of SDF-1, consistent with the lack of cell migration in animals without infarction (Fig. 3*N*). Clearly, the acute MI serves as a potent attractant for MPCs, supporting the use of local cell delivery in protocols targeting MI and heart failure. However, other signaling mechanisms could be involved, via constitutively released SDF-1, once the MPCs have entered the infarct bed.

Our delivery platform altered the SDF-1/CXCR4 expression in MPCs in such a way that favors cell migration into the infarct bed. Whole genome profiling revealed augmented CXCR4 expression and suppressed SDF-1 expression in TGF-β–conditioned MPCs in a composite scaffold, compared with the injected TGF-β–conditioned MPCs (Fig. 2*J*). This effect is significant for the therapeutic use of MPCs, because it results in increased cell responsiveness to a gradient of SDF-1. The MPCs within the composite scaffold do not secrete SDF-1, but instead migrate out and into the infarct bed toward high concentrations of SDF-1, due to their high expression of CXCR4. However, after the release of MPCs into the infarct bed, these cells are expected to recover their ability to secrete SDF-1 and further contribute to the SDF-1 gradient (Fig. 3 *Q* and *R*). Taken together, these data support the notion that the MSCs engineered to express high levels of CXCR4 could augment therapeutic angiogenesis (34). These effects were observed using a nude rat model of MI, as in our previous studies (47) because it provides the inflammatory signals associated with the progression of MI from acute to chronic, while alleviating rejection of implanted cells.

In summary, we describe a tissue engineering platform for cell therapy of MI comprising two components: cells (autologous or matched allogeneic cells derived from bone marrow, immunose-

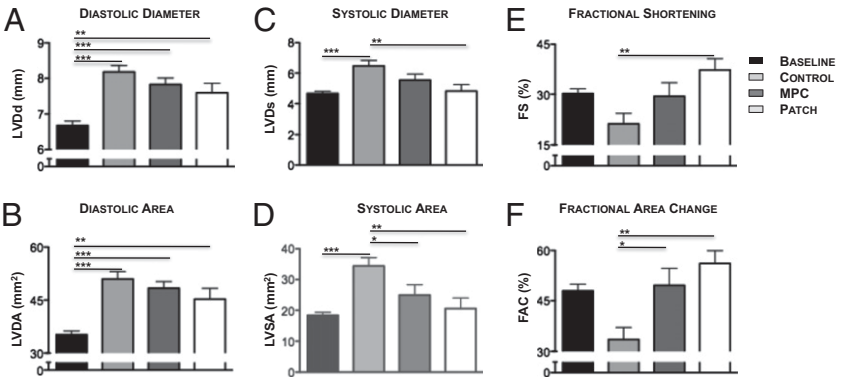

Fig. 4. Changes in left ventricular function after composite scaffold delivery. Baseline values (n = 45) measured at 3 d postinfarction in rats that subsequently received intramyocardial injection of MPCs (n = 15), composite construct (n = 15), or no intervention (n = 15). After an additional 4 wk, LVDd (*A*) and LVDA (*B*) showed little difference between groups, whereas LVDs (*C*) and LVSA (*D*) were preserved in the MPC-injected and patch-implanted groups. FS (*E*) and FAC (*F*) continued to decline in untreated controls and were well preserved by MPC injection and slightly more so by patch implantation. Data for individual animals are shown in Fig. S2.

lected and preconditioned with TGF-β) and a composite scaffold (decellularized human myocardium that is nonimmunogenic, combined with fibrin gel derived from the patient's blood). This adaptable modular platform can be tailored as necessary and extended to induced pluripotent stem cell–derived cardiomyocytes and vascular cells, as well as other hydrogels, such as hyaluronans (48). Ultimately, we envision this system as a possible point-of-care approach, with components produced and assembled to most effectively target signaling mechanisms involved in the repair process. TGF-β conditioning enhanced the vasculogenic properties of bone marrow-derived MPCs and expression of SDF-1, whereas the composite scaffold transiently decreased the expression of SDF-1 and increased the expression of CXCR4. Our data indicate that the TGF-β conditioning and the composite scaffold applied in sequence induced MPC migration into the infarct bed, where these cells recovered their ability to secrete SDF-1, which in turn enhanced further cell migration, revascularization of the infarct bed, and preservation of myocardial function.

Methods

The composite scaffold was constructed from fully decellularized human myocardium with preserved composition, structure, and mechanics of the extracellular matrix and fibrin hydrogel containing human mesenchymal stem cells that were conditioned in vitro using small concentrations of TGF-β. The composite was investigated in vitro and in a nude rat implantation model using molecular, structural, and functional assays. Detailed methods are provided in *SI Methods*.

Statistical Analysis. The experimental data were analyzed by multiway ANOVA followed by Tukey's post hoc analysis, using Statistica software. For the whole genome profiling, comparisons between experimental groups were performed using permutation analysis for differential expression. $P < 0.05$ was considered significant in all cases.

ACKNOWLEDGMENTS. We thank Angioblast Systems for providing human MPCs through a material transfer agreement with Columbia University and Ann Marie Schmidt for her insightful suggestions. This work was supported by National Institutes of Health Grants HL076485 and EB002520 (to G.V.-N.) and HL076485-04S1 (to A.G.-F.).

1. Bergmann O, et al. (2009) Evidence for cardiomyocyte renewal in humans. *Science* 324:98–102.
2. Martens TP, et al. (2006) Mesenchymal lineage precursor cells induce vascular network formation in ischemic myocardium. *Nat Clin Pract Cardiovasc Med* 3(Suppl 1):S18–S22.
3. Yang L, et al. (2008) Human cardiovascular progenitor cells develop from a KDR$^+$ embryonic stem cell–derived population. *Nature* 453:524–528.
4. Ford ES, et al. (2007) Explaining the decrease in U.S. deaths from coronary disease, 1980–2000. *N Engl J Med* 356:2388–2398.
5. Chachques JC, et al. (2008) Myocardial Assistance by Grafting a New Bioartificial Upgraded Myocardium (MAGNUM) Trial: Clinical feasibility study. *Ann Thorac Surg* 85:901–908.
6. Janssens S, et al. (2006) Autologous bone marrow–derived stem-cell transfer in patients with ST-segment elevation myocardial infarction: Double-blind, randomised controlled trial. *Lancet* 367:113–121.
7. Laflamme MA, Murry CE (2005) Regenerating the heart. *Nat Biotechnol* 23:845–856.
8. Lunde K, et al. (2006) Intracoronary injection of mononuclear bone marrow cells in acute myocardial infarction. *N Engl J Med* 355:1199–1209.
9. Meyer GP, et al. (2006) Intracoronary bone marrow cell transfer after myocardial infarction: Eighteen months' follow-up data from the randomized, controlled BOOST (BOne marrOw transfer to enhance ST-elevation infarct regeneration) trial. *Circulation* 113:1287–1294.
10. Schächinger V, et al.; REPAIR-AMI Investigators (2006) Intracoronary bone marrow–derived progenitor cells in acute myocardial infarction. *N Engl J Med* 355:1210–1221.
11. Hou D, et al. (2005) Radiolabeled cell distribution after intramyocardial, intracoronary, and interstitial retrograde coronary venous delivery: Implications for current clinical trials. *Circulation* 112(9 Suppl):I150–I156.
12. Mangi AA, et al. (2003) Mesenchymal stem cells modified with Akt prevent remodeling and restore performance of infarcted hearts. *Nat Med* 9:1195–1201.
13. Murry CE, et al. (2004) Haematopoietic stem cells do not transdifferentiate into cardiac myocytes in myocardial infarcts. *Nature* 428:664–668.
14. Purhonen S, et al. (2008) Bone marrow–derived circulating endothelial precursors do not contribute to vascular endothelium and are not needed for tumor growth. *Proc Natl Acad Sci USA* 105:6620–6625.
15. Jakab K, et al. (2008) Tissue engineering by self-assembly of cells printed into topologically defined structures. *Tissue Eng Part A* 14:413–421.
16. Gerecht S, et al. (2007) Hyaluronic acid hydrogel for controlled self-renewal and differentiation of human embryonic stem cells. *Proc Natl Acad Sci USA* 104:11298–11303.
17. Martens TP, et al. (2009) Percutaneous cell delivery into the heart using hydrogels polymerizing in situ. *Cell Transplant* 18:297–304.
18. Gilbert TW, et al. (2008) Repair of the thoracic wall with an extracellular matrix scaffold in a canine model. *J Surg Res* 147:61–67.
19. Gilbert TW, Stewart-Akers AM, Simmons-Byrd A, Badylak SF (2007) Degradation and remodeling of small intestinal submucosa in canine Achilles tendon repair. *J Bone Joint Surg Am* 89:621–630.
20. Ott HC, et al. (2008) Perfusion-decellularized matrix: Using nature's platform to engineer a bioartificial heart. *Nat Med* 14:213–221.
21. Robinson KA, et al. (2005) Extracellular matrix scaffold for cardiac repair. *Circulation* 112(9 Suppl):I135–I143.
22. Arts T, Costa KD, Covell JW, McCulloch AD (2001) Relating myocardial laminar architecture to shear strain and muscle fiber orientation. *Am J Physiol Heart Circ Physiol* 280:H2222–H2229.
23. Gronthos S, et al. (2007) A novel monoclonal antibody (STRO-3) identifies an isoform of tissue-nonspecific alkaline phosphatase expressed by multipotent bone marrow stromal stem cells. *Stem Cells Dev* 16:953–963.
24. Holderfield MT, Hughes CC (2008) Crosstalk between vascular endothelial growth factor, notch, and transforming growth factor-β in vascular morphogenesis. *Circ Res* 102:637–652.
25. Lebrin F, Deckers M, Bertolino P, Ten Dijke P (2005) TGF-β receptor function in the endothelium. *Cardiovasc Res* 65:599–608.
26. Ng F, et al. (2008) PDGF, TGF-β, and FGF signaling is important for differentiation and growth of mesenchymal stem cells (MSCs): Transcriptional profiling can identify markers and signaling pathways important in differentiation of MSCs into adipogenic, chondrogenic, and osteogenic lineages. *Blood* 112:295–307.
27. Psaltis PJ (2009) *The Cardiovascular Reparative Properties of Bone Marrow Mesenchymal Precursor Cells.* PhD thesis (Univ of Adelaide, Adelaide, Australia).
28. Psaltis PJ, et al. (2010) Enrichment for STRO-1 expression enhances the cardiovascular paracrine activity of human bone marrow–derived mesenchymal cell populations. *J Cell Physiol* 223:530–540.
29. See F, et al. Therapeutic effects of human STRO-3–selected mesenchymal precursor cells and their soluble factors in experimental myocardial ischemia. *J Cell Mol Med*, 10.1111/j.1582-4934.2010.01241.x.
30. Au P, Tam J, Fukumura D, Jain RK (2008) Bone marrow–derived mesenchymal stem cells facilitate engineering of long-lasting functional vasculature. *Blood* 111:4551–4558.
31. Shi S, Gronthos S (2003) Perivascular niche of postnatal mesenchymal stem cells in human bone marrow and dental pulp. *J Bone Miner Res* 18:696–704.
32. Gnecchi M, et al. (2006) Evidence supporting paracrine hypothesis for Akt-modified mesenchymal stem cell–mediated cardiac protection and functional improvement. *FASEB J* 20:661–669.
33. Passier R, van Laake LW, Mummery CL (2008) Stem-cell–based therapy and lessons from the heart. *Nature* 453:322–329.
34. Murry CE, Reinecke H, Pabon LM (2006) Regeneration gaps: Observations on stem cells and cardiac repair. *J Am Coll Cardiol* 47:1777–1785.
35. Zimmermann WH, et al. (2006) Engineered heart tissue grafts improve systolic and diastolic function in infarcted rat hearts. *Nat Med* 12:452–458.
36. Haider HKh, Jiang S, Idris NM, Ashraf M (2008) IGF-1–overexpressing mesenchymal stem cells accelerate bone marrow stem cell mobilization via paracrine activation of SDF-1α/CXCR4 signaling to promote myocardial repair. *Circ Res* 103:1300–1308.
37. Hu X, et al. (2007) Stromal cell–derived factor-1α confers protection against myocardial ischemia/reperfusion injury: Role of the cardiac stromal cell–derived factor-1α CXCR4 axis. *Circulation* 116:654–663.
38. Zhang M, et al. (2007) SDF-1 expression by mesenchymal stem cells results in trophic support of cardiac myocytes after myocardial infarction. *FASEB J* 21:3197–3207.
39. Grunewald M, et al. (2006) VEGF-induced adult neovascularization: Recruitment, retention, and role of accessory cells. *Cell* 124:175–189.
40. Askari AT, et al. (2003) Effect of stromal-cell–derived factor 1 on stem-cell homing and tissue regeneration in ischaemic cardiomyopathy. *Lancet* 362:697–703.
41. Avigdor A, et al. (2004) CD44 and hyaluronic acid cooperate with SDF-1 in the trafficking of human CD34$^+$ stem/progenitor cells to bone marrow. *Blood* 103:2981–2989.
42. De Visscher G, et al. (2010) The remodeling of cardiovascular bioprostheses under influence of stem cell homing signal pathways. *Biomaterials* 31:20–28.
43. Tang YL, et al. (2009) Hypoxic preconditioning enhances the benefit of cardiac progenitor cell therapy for treatment of myocardial infarction by inducing CXCR4 expression. *Circ Res* 104:1209–1216.
44. Dvir T, et al. (2009) Prevascularization of cardiac patch on the omentum improves its therapeutic outcome. *Proc Natl Acad Sci USA* 106:14990–14995.
45. Lee BC, et al. (2009) Cell therapy generates a favourable chemokine gradient for stem cell recruitment into the infarcted heart in rabbits. *Eur J Heart Fail* 11:238–245.
46. Penn MS (2009) Importance of the SDF-1:CXCR4 axis in myocardial repair. *Circ Res* 104: 1133–1135.
47. Radisic M, et al. (2008) Pre-treatment of synthetic elastomeric scaffolds by cardiac fibroblasts improves engineered heart tissue. *J Biomed Mater Res A* 86:713–724.
48. Sahoo S, Chung C, Khetan S, Burdick JA (2008) Hydrolytically degradable hyaluronic acid hydrogels with controlled temporal structures. *Biomacromolecules* 9:1088–1092.